Pablo Guindos

COMPARISON OF DIFFERENT FAILURE APPROACHES IN KNOTTY WOOD

This article presents and assesses 64 different ways for predicting the failure onset in knotty wooden beams. The aim is to provide engineers and modellers a general view of how to evaluate the failure in wooden structural members with knots. The studied criteria included both the conventional point-based and average stress theories. Special attention was paid to the effect of the elements of the wood mesostructure, i.e. knots and fiber deviation, which can generate singular stress concentrations as notches or cracks would do in fracture mechanics. The case study consisted of predicting the failure onset of bending in structural wooden beams. A previously validated finite element model was used in order to compute the hete-rogeneous stresses. It was found that the knots caused considerable stress singula-rities so that the size of the average stress theory influenced the failure predictions by up to 23%. However, the variations generated by distinct phenomenological criteria were in general much smaller. The application of the average stress theory in large stress integration volumes is strongly recommended when predicting the failure in wood members.

Introduction

Knots are considered defects in wood because they are the most strength-reducing components of this material [Phillips et al. 1981]. Indeed accounting for knots and fiber orientation in wooden numerical models is common practice. However, wood failure prediction is a complex topic due to structural complexity and hete-rogeneity. In literature, many approaches for timber failure criterion are available [Smith et al. 2003; Thelandersson, Larsen 2003; Kasal, Leichti 2005], but there is no agreement on which approach offers the best fit and what the main differences between each approach are. Usually these criteria are classified by their stochastic or deterministic bases, as well as whether or not fracture toughness is considered.

Pablo Guindos (*pablo.guindos@wki.fraunhofer*), Fraunhofer WKI – Institute for Wood Research, Braunschweig, Germany

The stochastic basis allows for a heterogeneous wood concept, and rupture is predicted by assessing the probability of failure in the weakest region. This approach can be applied in order to not only predict the failure load by itself, but also as a complement to other deterministic approaches with [Foschi et al. 1989; Gustafsson, Serrano 1999] or without [Clouston et al. 1998] fracture toughness considerations. Yet, statistical premises do not provide physical explanations concerning the rupture phenomenon, which is the main objective of numerical models.

Conversely, from the deterministic point of view, failure is predicted from the analysis of some physical variables which enables understanding of the rupture process. These variables are normally the stresses, strains, strengths, crack lengths, stress intensity factors, and energy release rates. The wood is usually modelled as a homogeneous continuum so that the failure load is predicted either by performing a conventional strength-based analysis with any of the multiple phenomenological failure criteria, if no initial notches or cracks are present, or by applying a crack growth criterion under the linear or non-linear fracture mechanics theories in the cases of singular stress concentrations. Nevertheless, other modelling paradigms [Smith et al. 2003], such as the heterogeneous finite element models, morphology-based models and lattice models, have achieved more precise emulations of the wood material. All these new paradigms have in common is that they account for the timber heterogeneity at various scales. However, it was demonstrated [Guindos, Guaita 2013] that conventional failure approaches (i.e. point-strength-based criterion and fracture mechanics) may not be appropriate for heterogeneous wooden models. This is because on the one hand the heterogeneous components of the wood structure (e.g. knots and fiber deviation) are capable of generating singular stress concentrations which reduce the accuracy of the point-strength-based criteria while on the other hand, the number and location of heterogeneities in each specimen seriously hampers the application of fracture mechanics approaches.

Nevertheless, the theory of the small finite area [Masuda 1988] or the mean stress approach [Landelius 1989; Aicher et al. 2002] may circumvent the aforementioned limitations. These approaches consist of computing the average stresses of an area or volume (stress integration region) to further apply a conventional phenomenological failure criterion. Thus, a priori stress identification is not required and may be suitable in the event of stress singularities. This may considerably enhance the usability of current wooden numerical models

Since previous research only emphasized the application of conventional point-strength-based criteria in 2 [Aicher, Klöck 2001; Garab, Szalai 2010] and 3-D [Murray 2007] homogeneous models, the objective of this research was to assess the applicability of these new approaches and compare them to conventional criteria. As a result, a comparison of 64 different ways to predict the failure load in wood is presented and analysed.

Background to phenomenological failure criteria

This section briefly introduces the phenomenological failure criteria that were considered in this research.

Tsai-Hill Criterion

Tsai [1965] proposed the following equation for composite materials from the criterion proposed by Hill [1948]:

$$A(\sigma_L - \sigma_R)^2 + B(\sigma_R - \sigma_T)^2 + C(\sigma_T - \sigma_L)^2 + D\tau_{LR}^2 + E\tau_{RT}^2 + F\tau_{LT}^2 = 1 \quad (1)$$

where: σ_L, s_R, s_T, τ_{LR}, τ_{RT} and τ_{TL} – the uniaxial and shearing stress components in the respective directions and sections,
A, B, C, D, E and F – coefficients dependent upon the uniaxial and shearing strengths.

This criterion does not account for differences between the tensile and compressive strengths, therefore average strengths must be used instead.

Tsai-Azzi Criterion

Later, Tsai and Azzi [1966] simplified the Tsai-Hill criterion for plane stress conditions, demonstrating its applicability for composites with different strengths in tension and compression, by changing the uniaxial strengths according to the sign of the stresses:

$$\frac{\sigma_L{}^2}{f_L{}^2} - \frac{\sigma_L\sigma_R}{f_L{}^2} + \frac{\sigma_R{}^2}{f_R{}^2} + \frac{\tau_{LR}{}^2}{f_{LR}{}^2} = 1 \quad (2)$$

where: f_L, f_R and f_{LR} – the uniaxial and shearing strengths relative to the corresponding wood directions and sections.

As reported by Nahas [1986], Tsai also developed two additional equations for the two other mutually orthogonal planes by interchanging the subscripts L-R for L-T and R-T in eq.2.

Norris Criterion

Norris [1962] performed a specific evaluation for wood, developing a criterion very similar to Tsai-Azzi except that the interaction terms were not biased towards one particular strength:

$$\frac{\sigma_L{}^2}{f_L{}^2} - \frac{\sigma_L\sigma_R}{f_L f_R} + \frac{\sigma_R{}^2}{f_R{}^2} + \frac{\tau_{LR}{}^2}{f_{LR}{}^2} = 1 \quad (3)$$

Similarly, by interchanging the L-R subscripts and signs, it is possible to distinguish among the planes, and tensile and compressive strengths.

Extended Yamada-Sun Criterion

Yamada and Sun [1978] proposed a plane stress criterion similar to the previous two, except that it only calculates the normal and shearing stresses. As reported by Murray [2007], this criterion can be extended to three-dimensional models by adding the transverse shearing term in each direction:

$$\frac{\sigma_L{}^2}{f_L{}^2} + \frac{\tau_{LR}{}^2}{f_{LR}{}^2} + \frac{\tau_{LT}{}^2}{f_{LT}{}^2} = 1 \tag{4}$$

hence, according to the above expression, 12 equations have to be derived.

Hoffman Criterion

Hoffman [1967] proposed 3 linear terms in the Hill criterion so that it is possible to distinguish among the tensile-compressive strengths using only one equation:

$$A(\sigma_L - \sigma_R)^2 + B(\sigma_R - \sigma_T)^2 + C(\sigma_T - \sigma_L)^2 + D\tau_{LR}^2 + E\tau_{RT}^2 + F\tau_{LT}^2 + G\sigma_L \\ + H\sigma_R + I\sigma_T = 1 \tag{5}$$

where: A,B,…,I – coefficients dependent upon shearing and uniaxial compressive and tensile strengths.

Hashin Criterion

The Hashin [1980] criterion discerns 4 modes of failure, including:

parallel tension:

$$\frac{\sigma_L{}^2}{f_{t,0}{}^2} + \frac{\tau_{LR}{}^2 + \tau_{LT}{}^2}{f_{v,0}{}^2} = 1 \tag{6}$$

parallel compression:

$$\frac{\sigma_L}{f_{c,0}} = 1 \tag{7}$$

perpendicular tension:

$$\frac{(\sigma_R + \sigma_T)^2}{f_{t,90}{}^2} + \frac{\tau_{RT}{}^2 - \sigma_R\sigma_T}{f_{v,90}{}^2} + \frac{\tau_{LR}{}^2 + \tau_{LT}{}^2}{f_{v,0}{}^2} = 1 \tag{8}$$

and perpendicular compression:

$$\frac{(\sigma_R + \sigma_T)^2}{4f_{v,0}^2} + \left[\left(\frac{f_{c,90}}{2f_{v,90}}\right)^2 - 1\right]\frac{(\sigma_R + \sigma_T)^2}{f_{c,90}^2} + \frac{\tau_{RT}^2 - \sigma_R\sigma_T}{f_{v,90}^2} + \frac{\tau_{LR}^2 + \tau_{LT}^2}{f_{v,0}^2} = 1 \quad (9)$$

where: $f_{t,0}$, $f_{c,0}$, $f_{t,90}$, $f_{c,90}$, $f_{v,0}$ and $f_{v,90}$ are, respectively, the strengths related to longitudinal tension and compression, transverse tension and compression and longitudinal and transverse shearing.

Tsai-Wu Criterion

Tsai and Wu [1971] developed a tensor polynomial strength criterion from Goldenblat and Kopnov's theory. For transversely isotropic models, the Tsai-Wu criterion can be formulated as follows:

$$F_1\sigma_L + F_2(\sigma_R + \sigma_T) + F_{11}\sigma_L^2 + F_{22}(\sigma_R^2 + \sigma_T^2 + 2\tau_{RT}^2) + F_{66}(\tau_{LR}^2 + \tau_{LT}^2) + 2F_{12}(\sigma_L\sigma_R + \sigma_L\sigma_T) + 2F_{23}(\tau_{RT}^2 - \sigma_R\sigma_T) = 1 \quad (10)$$

where: F_1, F_2, F_{11}, F_{22}, F_{66} and F_{23} are coefficients obtained from shearing and uniaxial strengths. F_{12} is a coefficient which, on the one hand represents the biaxial wooden strength in the longitudinal and transverse directions, and on the other, ensures the mathematical consistency of eq. 10 when the following condition is satisfied:

$$F_{12} = \frac{2}{f_{t,45}^2}(1 - \frac{f_{t,45}}{2}\left(\frac{1}{f_{t,0}} - \frac{1}{f_{c,0}} + \frac{1}{f_{t,90}} - \frac{1}{f_{c,90}}\right)$$
$$- \frac{f_{t,45}^2}{4}\left(\frac{1}{f_{t,0}f_{c,0}} + \frac{1}{f_{t,90}f_{c,90}} + \frac{1}{f_{v,0}^2}\right)) \quad (11)$$

Much controversy involves the determination of F_{12} in the wood. Originally, Tsai and Wu proposed the following equation to compute F_{12} from 45-degree off-axis tensile tests:

$$F_{12} = \frac{1}{2}\left(\frac{1}{f_{t,0}f_{c,90}} + \frac{1}{f_{c,0}f_{t,90}} - \frac{1}{f_{v,0}^2}\right) \quad (12)$$

where $f_{t,45}$ is the 45-degree off-axis tensile strength.

Another method for calculating F_{12} was proposed by Liu [1984]:

$$F_{12} = \frac{1}{2}\left(\frac{1}{f_{t,0}f_{c,90}} + \frac{1}{f_{c,0}f_{t,90}} - \frac{1}{f_{v,0}^2}\right) \quad (13)$$

Background on the average stress approach

The average (or mean) stress approach consists of calculating the mean stresses of a certain region in a phenomenological failure criterion rather than the singular stresses of discrete points. The reason for this is to obtain the advantages of both the phenomenological criteria and the fracture mechanics approach within the same method. On the one hand, the phenomenological failure criteria are simple and can be applied to heterogeneous media because they do not require a priori identification of cracks or singularities. On the other hand, the size of the region of the average stress approach is chosen from fracture mechanics considerations so that, in the case of singular stress concentrations, this approach generates similar failure loads to those of the fracture mechanics approaches.

The key aspects of this average approach are the phenomenological criterion and the size of the stress integration region. Two different approaches to this theory have been developed to date. Firstly, Masuda [1988] suggested that the integration size was related to the size of the wooden fibers. This researcher concluded that the proper size was a regular hexahedron of $1 \times 0.4 \times 0.4$ mm to $2 \times 0.4 \times 0.4$ mm, corresponding to the L, R and T directions, respectively. This conclusion was obtained after calculating the theoretical stresses of notched beams [Masuda 1986], GOST specimens [Masuda 1988] and shear tests [Masuda 1994] in the Norris criterion, and comparing experimental with numerical results. Secondly, Landelius [1989] deduced the proper integration size (x_0) from a theoretical point of view. This was achieved by relating the stress at the front of a sharp crack with the transverse tensile strength and the critical strain energy release rate for mode I of rupture (G_{IC}):

$$x_0 = \frac{2E_I G_{IC}}{\pi f_{t,0}{}^2} \tag{14}$$

where E_I is the equivalent orthotropic stiffness for mode I of rupture, which relates the stress intensity factor with the energy release rate and depends on the in-plane elastic parameters [Paris, Sih 1965]. Subsequently, Aicher et al. [2002] extended this approach for mixed (mode I and II) failures. This was done by correlating theoretical axial and shearing stresses, the Norris criterion and critical strain energy release rates. Thus, the integration size is given by:

$$x_0 = \frac{2E_I G_{IC}}{\pi f_{t,0}{}^2} \frac{E_x}{E_y} \left(\frac{G_{IIC}}{G_{IC}}\right)^2 \frac{1}{4k^4} \left\{ \sqrt{1 + 4k^2 \sqrt{\frac{E_y}{E_x}} \frac{G_{IC}}{G_{IIC}}} - 1 \right\}^2 \left\{ 1 + \frac{k^2}{\left(f_{v,0}/f_{t,0}\right)^2} \right\} \tag{15}$$

where: E_x, E_y – respectively, the longitudinal and transverse elastic moduli,

      G_{IIC} – the critical energy release rate for mode II of rupture,

      k – the mixed mode ratio or relationship between the average shear and normal stresses (τ/σ).

The application of this equation to heterogeneous timber becomes difficult because of the varying mixed mode ratio (k).

Although the same phenomenological failure criterion (Norris) was used in both theories, the typical integration sizes given by eq.15 range from 4 to 20 mm in softwoods [Thelandersson, Larsen 2003] which are very different from those dimensions proposed by Masuda.

Materials and methods

In order to compare the different failure approaches, a validated numerical model was considered [Guindos, Guaita 2013]. This model was constructed with ANSYS Multiphysics v11 (ANSYS Inc., Canonsburg, PA, USA), and accounted for the heterogeneity (knots and fiber orientations) of 9 *P. sylvestris* structural beams of 3000 × 150 × 50 mm, which were experimentally tested in a standard 4 point bending test [DIN EN 408: 2010] (fig. 1). The main characteristics of this model are described below – however, the reader is referred to Guindos and Guaita [2013] for a thorough explanation of the model.
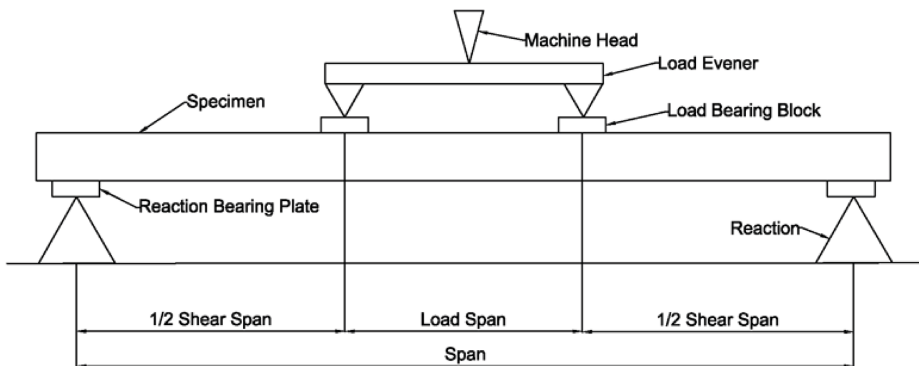

Fig. 1. 4-point bending test layout

The 3D geometry of the knots was modelled as oblique elliptical cones. Fig. 2 illustrates this geometry, and presents the necessary measuring parameters.
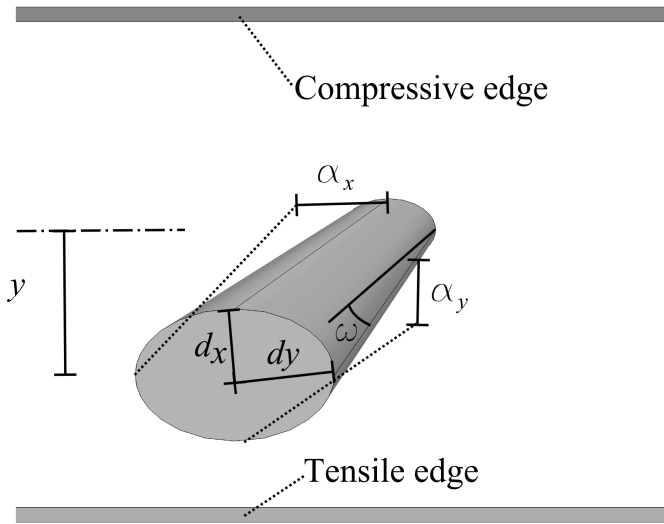
Fig. 2. Geometry of the knots in the model, including the measuring parameters: position (y), minor (d_x) and major (d_y) semi-axis, conical angle (ω), and vertical (a_y) and horizontal (a_x) inclinations

The global fiber orientation was calculated by applying the theory of flow-grain analogy [Phillips et al. 1981] in 3D. The flow-grain theory consists of establishing equivalence between the streamlines of a laminar flow and the fibre orientation in the wood, see fig. 3. This theory presents the advantage that, once the geometry of the knots is defined, the fiber orientations are calculated according to the equations of fluid dynamics and therefore no experimental measurement is needed. The practical application of this theory in the present model is summarized in 7 steps: (1) the geometry of the beam and knots was defined; (2) a prismatic pipe enveloping the beam and knots was created; (3) the bases of this pipe (located close to the ends of the beam) were defined as the inlet (small velocity) and outlet (atmospheric pressure) boundary conditions for a laminar flow; (4) the remaining surfaces of the pipe and the external surfaces of the knots were defined as non-slip (wall) boundary conditions (i.e. zero velocity); (5) the whole domain was meshed and the equations of laminar fluid dynamics were solved, providing the streamlines (velocity vectors) of the fluid in the whole domain; (6) the elements of the pipe were deleted and only the elements of the beam were retained; (7) the elements of the pipe were transformed to solid elements and the material (fiber) orientation was assumed to be equal to that of the previously calculated velocity vector – this made it possible to consider the fibers' orientation in the model. A conventional solid analysis was then performed, and the stress field was calculated. It is worth mentioning that given the complexity of the fiber orientation (fig. 3), the stress field of the case study was extremely heterogeneous even under homogeneous loading conditions. Indeed, all the stress components were present around the knots [Guindos, Guaita 2014].

With regard to the solid calculations, the wood was modelled as a transversely isotropic material with anisotropic plasticity. The plastic algorithm consisted of the initial yield surface of Hill [1948], the generalizations of Shih and Lee [1978] and the hardening model of Valliappan et al. [1976]. The uniaxial and shearing strengths of the species used were taken from literature [Boström 1992; Argüelles 1994; Thelandersson, Larsen 2003; Grekin 2006] and are shown in table 1.
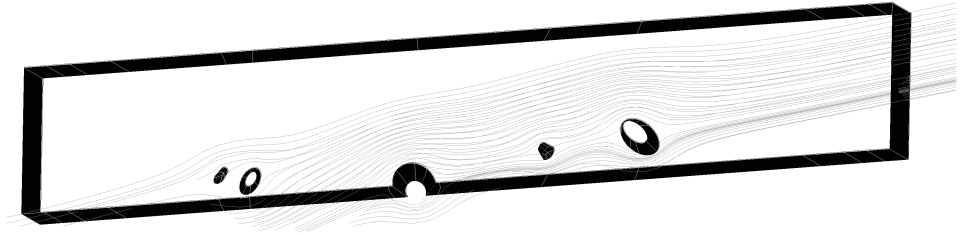

Fig. 3. Fiberorientation according to flow-grain analogy. The figure shows the load span (see fig. 1.) of a beam including the knots and the fiber orientation. The fiber orientation is accounted for in the model by simulating a laminar flow around the knots and reorienting the orthotropic directions

Table 1. Strengths of *P. sylvestris* used in this study

Strength	Value [N/mm^2]
Longitudinal tension ($f_{t,0}$)	89.0
Longitudinal compression ($f_{c,0}$)	57.0
Transverse tension ($f_{t,90}$)	4.0
Transverse compression ($f_{c,90}$)	7.6
Longitudinal shear ($f_{v,0}$)	9.5
Transverse shear ($f_{v,90}$)	13.3
45 off-axis tension ($f_{t,45}$)	4.5

The accuracy of the model was tested against structural bending tests [DIN EN 408: 2010]. As verified by a digital image correlation analysis (DIC), all the beams failed due to the influence of the knots located at the tensile region of the load span. The measuring parameters of the failure knots are presented in table 2. The validation of the model consisted of comparing 65 FE nodal displacements in each member against DIC. The location and load of failure were also compared with the numerical predictions, see fig. 4. The photogrammetric technique made it possible to consider the influence of the knots in the elastic modulus [Guindos, Ortiz 2013]. The failure prediction errors of the model were up to 4%, the failure location was predicted with an accuracy of less than 20 mm, and the accuracy of the displacement field was 9%.

a

b

c

d

e

Global error = 5.75%, Error in knotty areas = 5.83%
Error defect - free areas = 5.68%

■ Load = 0 kN   ◇ Load = 5.888 kN Photogrammetry
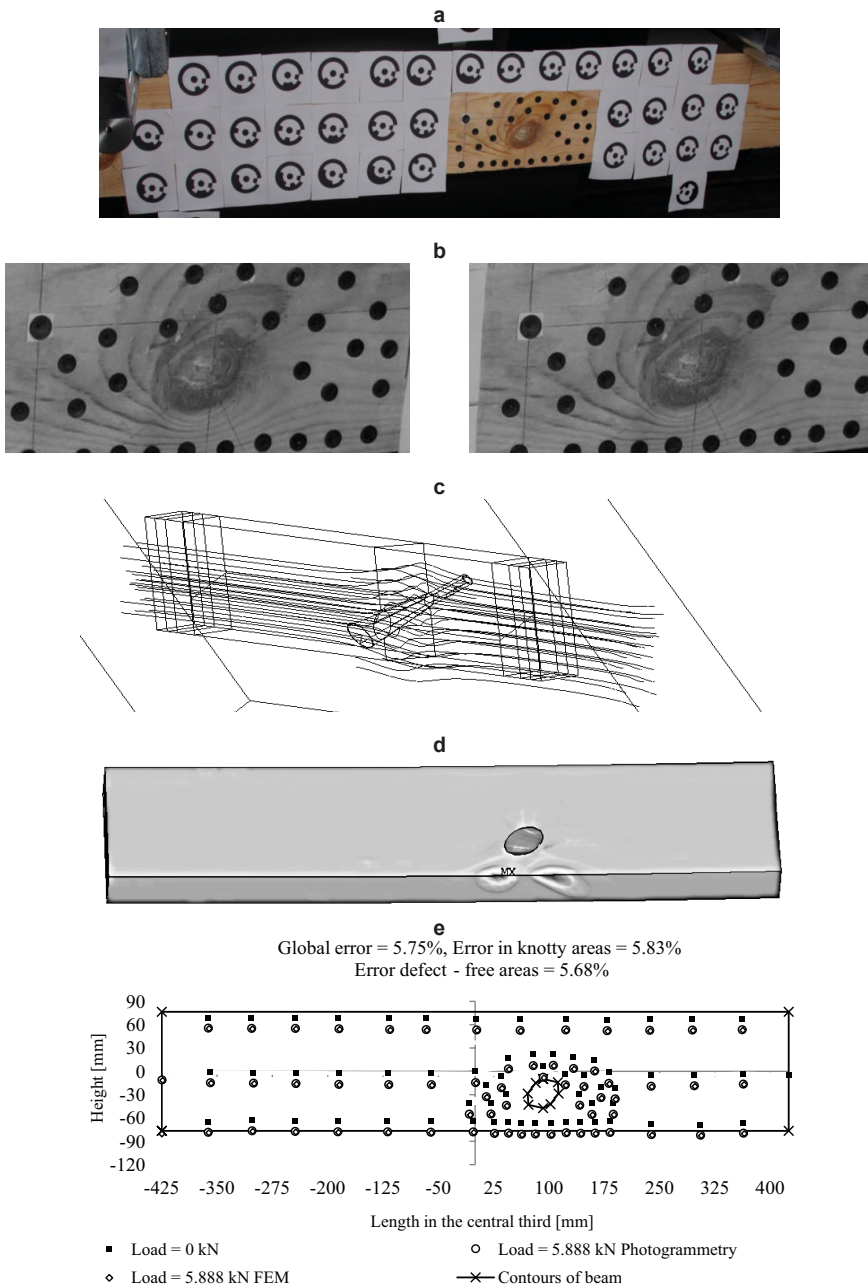◇ Load = 5.888 kN FEM   ✕ Contours of beam

Fig. 4. Experimental and numerical validation. (a) Photogrammetric measuring points in each beam. (b) Detection of knot, location and load of failure via image correlation. (c) Numerical simulation of knot of failure and grain deviation. (d) Calculation of failure criteria (Hoffmann criterion shown in the image). (e) Comparison of photogrammetric versus numerical displacements

Table 2. Characteristics of the failure knots, including the measuring parameters: position (y), minor (d_x) and major (d_y) semi-axis, conical angle (ω), and vertical (a_y) and horizontal (a_x) inclinations.

Beam	Knot size [mm]		Position [mm]	Conical angle [deg]	Inclination [mm]	
	d_x	d_y	y	w	a_x	a_y
1	16	18	-21	9	22	-2
2	17	22	-38	3	-49	-16
3	20	24	-24	6	43	5
4	24	30	-13	11	18	7
5	16	17	-43	15	27	16
6	17	25	-28	20	56	29
7	19	30	-38	20	39	25
8	24	35	-11	24	-61	20
9	12	22	-51	7	110	-35

Once the model was validated, the different failure criteria were compared. This comparison included all the previous phenomenological failure criteria, i.e. Tsai-Hill, Tsai-Azzi, Norris, extended Yamada-Sun, Hoffmann, Hashin and Tsai-Wu. The Tsai-Wu criterion was applied twice with distinct interaction coefficients F_{12}. The first coefficient was calculated according to eq. 12, and the second according to eq. 13, which in this case corresponded, respectively, to the maximum and minimum values to ensure the mathematical consistency of the Tsai-Wu criterion (eq. 11). This research therefore investigated the extreme values according to the Tsai-Wu predictions according to F_{12}.

Table 3. Size of the stress integration volumes used to proceed with the average (mean) stress approach

Length [mm]		
L-axis	R-axis	T-axis
10	10	10
8	8	8
6	6	6
4	4	4
2	2	2
2	0.4	0.4
1	0.4	0.4
0 (Nodal)	0 (Nodal)	0 (Nodal)

In addition, these 8 distinct phenomenological criteria were applied according to 8 different approaches. Firstly, the conventional point stress-based criterion

was considered, i.e. the stresses that are calculated in the different criteria correspond to the calculated stresses at the FE integration points (of $2 \times 2 \times 2$ mm elements). The 7 remaining approaches consisted of integrating the stresses in different hexaedric volumes in order to apply the average (mean) stress approach (table 3).

Results and discussion

The failure predictions and errors of the different approaches and criteria are shown in table 4 for stress integration volumes of $10 \times 10 \times 10$ mm. The average errors of all the approaches are shown in fig. 5. In the case study, the best failure prediction was provided by the Tsai-Hill criterion when calculated in stress integration volumes of $8 \times 8 \times 8$ mm in size, with an absolute error of 4.14%.

Table 4. Average errors in failure prediction according to the different (a) phenomenological failure criteria and (b) average stress approaches

Beam	Failure Load [kN]	Numerical Error [%]							
		Tsai-Wu a	Hashin	Hoffman	Norris	Tsai-Azzi	Tsai-Hill	Tsai-Wu b	Yamada-Sun
1	13.9	-9.3	11.6	7.3	6.7	-0.7	3.3	23.8	5.8
2	11.5	-16.5	0.4	-3.0	-0.4	-7.4	-2.6	12.6	1.30
3	11.4	-10.8	9.0	4.6	6.3	-1.6	3.3	22.1	7.7
4	11.4	-9.7	9.1	6.5	9.1	1.2	6.1	24.0	10.9
5	11.3	-9.8	8.3	7.0	11.4	3.5	6.5	20.7	8.8
6	13.5	-32.4	-18.3	-8.0	0.5	-6.5	-7.2	-5.4	-9.8
7	12.6	-25.3	-12.2	-13.4	-9.4	-15.7	-8.2	0.6	-11.4
8	14.3	-20.7	-5.3	1.1	7.4	3.5	4.9	10.9	-1.8
9	13.0	-30.5	-14.0	-2.8	3.7	3.7	1.4	16.7	1.8
Absolute error [%]		18.3	9.8	6.0	6.1	4.9	4.8	15.2	6.6
Average error [%]		-18.3	-1.3	-0.1	4.0	-2.2	0.8	14.0	1.5
Maximum error [%]		32.4	18.3	13.4	11.4	15.8	8.2	24.0	11.4
Standard deviation [%]		9.3	11.5	7.3	6.3	6.5	5.7	10.5	7.9

[a] F_{12} according to experimental values eq. 12
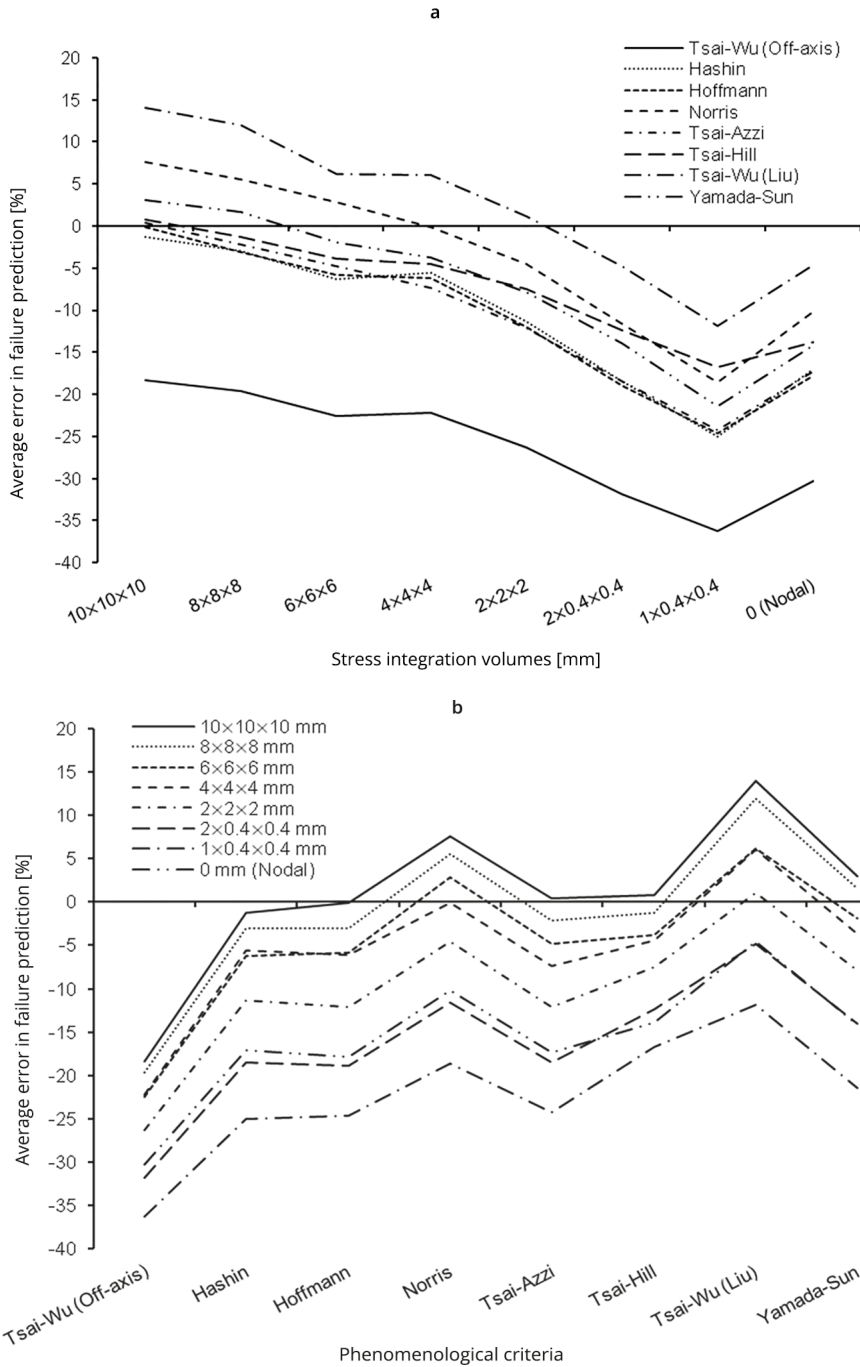[b] F_{12} according to Liu theory eq. 13

Fig. 5. Average errors in failure prediction according to the different (a) phenomeno-logical failure criteria and (b) average stress approaches

Discussion of the phenomenological failure criteria

As shown in fig. 4. a, all the phenomenological criteria remained quasi parallel through the different approaches. The Tsai-Wu criterion, according the 45-degree off-axis tensile test, which represented the maximum value of the interaction factor (F_{12}), provided the most conservative predictions, ranging between –36 and –18% of the actual value of the failure load. Thus the size effect of the stress integration volume was approximately 18% for this criterion. The most accurate stress integration volume was 10 × 10 × 10 mm, which was the largest size, therefore the lowest sensitivity to singular stress concentrations was observed. The calculation of this criterion was simple because the strength differences in tension and compression were taken into account by only one robust equation. It did not provide information about the cause of failure, however, and as can be appreciated in fig. 4. a, the importance of the interaction factor (F_{12}) was crucial, therefore this uncertainty may be a considerable shortcoming.

The criteria of Hoffman, Hashin and Tsai-Azzi provided similar errors, ranging from –24 to 0%. The size effect was 24%, 6% higher than those the effect for the Tsai-Wu criterion. Again, the best integration size was 10 × 10 × 10 mm for all of these criteria. The necessary number of equations was 1, 4 and 12, respectively, therefore the computational complexity increased. However, the Hoffman criterion did not allow immediate failure identification, while Hashin permitted parallel-perpendicular and tensile-compressive failure identification, and Tsai-Azzi provided information on the failure plane.

The extended Yamada-Sun and Norris criteria were almost parallel to the previous ones and showed a similar size effect, but the failure prediction was slightly less conservative, with errors from –21 to 3% and from –19 to +7%, respectively. The best integration size was 8 × 8 × 8 mm for the Yamada-Sun extended and 6 × 6 × 6 mm for the Norris criterion. In a similar way to the Tsai-Azzi theory, 12 equations were derived in each case, which provided detailed information about failure.

The Tsai-Hill criterion, most likely due to the lack of distinction between the tensile and compressive strengths, was not in line with the other criteria. When the stress integration sizes were larger than 4 × 4 × 4 mm, the predictions were very similar to Hoffman, Hashin or Tsai-Azzi. However, for smaller volumes, the predictions were akin to Norris or Yamada-Sun extended. The Tsai-Hill criterion provided an error between –17 and 5%, which means a size effect of 22%. This criterion provided accurate predictions, with only one equation. However, differences in tension and compression were not taken into account, and no information about the cause of failure was provided.

The Tsai-Wu criterion, according to the theory of Liu (minimum value of the interaction factor F_{12}), generated the least conservative predictions, providing errors from –12 to 14% (a similar size effect to the previous criteria). The predic-

tions were far less conservative than those provided by the experimental F_{12}. The optimum integration size was $2 \times 2 \times 2$ mm. There was therefore significant influence of the F_{12}, in that the predictions ranged between 24 and 32% higher than the values obtained with the maximum F_{12}. This demonstrated the great variability of the Tsai-Wu criterion according to the coefficient F_{12}.

Discussion of stress integration volumes

The results from the different stress integration volumes were parallel to each other, see fig. 4. b. As expected, failure prediction increased with stress integration size. The average prediction of all the phenomenological criteria ranged from –22.4 (for the smallest Masuda size $1 \times 0.4 \times 0.4$ mm) to –0.7% (for the 10 mm size). Overall, a decrease from 6 to 2% was observed between consecutively-sized volumes. The average prediction of the point strength-based criteria was 5.6% lower than its corresponding stress integration volume ($2 \times 2 \times 2$ mm). However, note that this stress integration volume involved a very fine mesh, therefore larger differences may be expected for coarser meshes.

Regarding the phenomenological failure criteria, the best fits were observed by: (1) the Tsai-Wu criterion according to the theory of Liu for the point strength-based criterion and Masuda's sizes with the 2 mm volumes; (2) the Norris criterion for 4 mm volumes; (3) the Yamada-Sun criterion for 6 mm volumes; (4) the Tsai-Hill criterion for 8 mm volumes; (5) the Tsai-Azzi criterion for 10 mm volumes.

According to these results, the average size effect in all the phenomenological failure criteria due to the heterogeneity of the wood was approximately 23%. Therefore, the failure prediction can 25% higher if the integration size varies from the smallest ($1 \times 0.4 \times 0.4$ mm) to the largest ($10 \times 10 \times 10$ mm) integration volume. Conversely, the effect of the different phenomenological criteria, excluding the Tsai-Wu criterion, was only approx. 8%. This variation raised to 28% with the Tsai-Wu criterion, but it should be considered that the extreme interaction factors F_{12} were accounted for in the case study.

Conclusion

Current numerical models of wood material make it possible to account for some structural heterogeneity at various scales such as knots or grain deviations. These models provide more precise numerical simulations but the application of conventional failure approaches (e.g. point strength criterion and fracture mechanics) becomes either less accurate or extremely difficult. However, the average (mean) stress approach may overcome such limitations and effectively implement current models. In this research, the application of the average stress approach on heterogeneous FE models, along with multiple phenomenological failure criteria, was presented and assessed.

The average stress theory correctly implemented the model used in the case study, which accounted for knots and grain deviation in 3D. Due to singular stress concentrations, the application of this theory, rather than the conventional point--strength analysis is strongly recommended in heterogeneous models. By applying this, the numerical predictions were found to be much more robust, especially if large volumes were taken into account (e.g. side lengths of 8 or 10 mm).

The size effect of different integration stress volumes was approximately 23% for the case study. However, it is suggested that sharper stress concentrations than the ones modelled in this research may arise from special types of knots (e.g. when several conical knots connect with each other at the edges of a member) which may increase the size effect. Therefore, the use of conservative criteria in larger volumes is recommended in order to make more robust models. The differences between the phenomenological failure criteria were, in general, lower than the differences among the consecutive volumes (8%). However, notable differences were found for the case of the Tsai-Wu failure criterion according to distinct interaction factors (F_{12}). In the event that this criterion is applied to wood, an exhaustive study of F_{12} should be performed. In any case, the use of at least 2-3 different criteria is recommended. The choice should be made according to the selected size of the stress integration volumes, and what information is required regarding the failure cause.

References

Aicher S., Klöck W. [2001]: Linear versus quadratic failure criteria for in-plane loaded wood based panels. Otto-Graf-Journal 12: 187–199

Aicher S., Gustafsson P.J., Haller P., Petersson H. [2002]: Fracture mechanics models for strength analysis of timber beams with a hole or a notch. Report of RILEM TC-133, Division of Structural Mechanics, Lund University, Lund

Argüelles B. [1994]: Animated simulation of wood piece behaviour. Dissertation (in Spanish), Polytechnic University of Madrid, Madrid

Boström L. [1992]: Method for determination of the softening behavior of wood and the applicability of a non linear fracture mechanics model. Dissertation, Lund University, Lund

Clouston P., Lam F., Barrett J.D. [1998]: Incorporating size effects in the Tsai-Wu strength theory for douglas-fir laminated veneer. Wood Science and Technology 32 [3]: 215–226

Foschi R.O., Folz B.R., Yao F.Z. [1989]: Reliability-based design of wood structures. Structural Research Series, Report No. 34, Department of Civil Engineering, University of British Columbia, Vancouver

Garab J., Szalaj J. [2010]: Comparison of anisotropic strength criteria in the biaxial stress state. Drewno 53 [183]: 51–66

Grekin M. [2006]: Nordic Scots pine vs. selected competing species and non-wood substitute materials in mechanical wood products – Literature survey. Working Papers of the Finnish Forest Research Institute 36, Finnish Forest Research Institute, Helsinki

Guindos P., Guaita M. [2013]: A three-dimensional wood material model to simulate the behavior of wood with any type of knot at the macro-scale. Wood Science and Technology 47 [43]: 585–599

Guindos P., Guaita M. [2014]: The analytical influence of all types of knots on bending. Wood Science and Technology 48 [3]: 533–552

Guindos P., Ortiz J. [2013]: The utility of low-cost photogrammetry for stiffness analysis and finite-element validation of wood with knots in bending. Biosystems Engineering 114 [2]: 86–96

Gustafsson P.J., Serrano E. [1999]: Fracture mechanics in timber engineering – some methods and applications. Proceedings of 1st RILEM Symposium on Timber Engineering, Stockholm: 141–150

Hashin Z. [1980]: Failure criteria for unidirectional fiber composites. Journal of Applied Mechanics-T ASME 47 [2]: 329–334

Hill R. [1948]: A theory of the yielding and plastic flow of anisotropic metals. Philosophical Transactions of the Royal Society A 193 [1033]: 281–297

Hoffman O. [1967]: The brittle strength of orthotropic materials. Journal of Composite Materials 1 [2]: 200–206

Kasal B., Leichti R.J. [2005]: State of the art in multiaxial phenomenological failure criteria for wood members. Progress on Structructural Engineering Materials 7 [1]: 3–13

Landelius J. [1989]: Finite area method. Report TVSM 5043, Division of Structural Mechanics, Lund University, Lund

Liu J.Y. [1984]: Evaluation of the tensor polynomial strength theory for wood. Journal of Composite Materials 18 [3]: 216–226

Masuda M. [1986]: Theoretical consideration on fracture criteria of wood. Bulletin of the Kyoto University Forestry 58: 241–250

Masuda M. [1988]: Theoretical consideration on fracture criteria of wood-Proposal of a finite small area theory. Proceedings of the WCTE 1988, Seattle, Vol 2, pp. 584–595

Masuda M. [1994]: Theoretical consideration on fracture criteria of wood-Proposal of non--linear finite small area fracture criterion. Proceedings of PTEC 1988, Gold Coast, Vol 2, pp. 479–485

Murray I. [2007]: Manual for LS-DYNA wood material model 143, Turner-Fairbank Highway Research Center, APTEK Inc., Lake Plaza Drive Springs, Colorado

Nahas M.N. [1986]: Survey of failure and post-failure theories of laminated fiber-Reinforced composites. Journal of Composites, Technology and Research 8 [4]: 138–153

Norris C.B. [1962]: Strength of orthotropic materials subjected to combined stresses. US Forest Products Laboratory, Report No. 1816, Madison, WI

Paris P.C., Sih G.C. [1965]: Stress analysis of cracks. ASTM Special Technical Publication STP 381: 30–80

Phillips G.E., Bodig J., Goodman J.R. [1981]: Flow grain analogy. Wood Science 14 [2]: 55–64

Shih C.F., Lee D. [1978]: Further developments in anisotropic plasticity. Journal of Engineering Materials and Technology 100 [3]: 294–302

Smith I., Landis E., Gong M. [2003]: Fracture and fatigue in wood, first ed. Wiley, West Sussex

Thelandersson S., Larsen H.J. [2003]: Timber engineering, first ed. Wiley, West Sussex.

Tsai S.W. [1965]: Strength characteristics of composite materials. NASA Report No. CR-224, Washington DC

Tsai S.W., Azzi V.D. [1966]: Strength of laminated composite materials. AIAA Journal 4 [2]: 296–301

Tsai S.W., Wu E.M. [1971]: A general theory of strength for anisotropic materials. Journal of Composite Materials 5 [1]: 58–80

Valliappan S., Boonlaulohr P., Lee I.K. [1976]: Non-linear analysis for anisotropic materials. International Journal of Numerical Methods in Engineering 10 [3]: 597–606

Yamada S.E., Sun C.T. [1978]: Analysis of laminate strength and its distribution. Journal of Composite Materials 12 [3]: 275–284

List of standards

DIN EN 408 [2010]: Timber structures – Structural timber and glued laminated timber – Determination of some physical and mechanical properties

Acknowledgements